FEBS Letters 425 (1998) 234–238 FEBS 20006

Solution conformation of an ET_B selective agonist, ET-1[Cys(Acm)^{1,15},Ala^3,Leu^7,Aib^{11}], in CD_3OH/H_2O by ^1H NMR and molecular modelling

Chandralal M. Hewage, Lu Jiang, John A. Parkinson, Robert Ramage, Ian H. Sadler*

Department of Chemistry, University of Edinburgh, West Mains Road, Edinburgh EH9 3JJ, UK

Received 3 February 1998

Abstract To understand the basic structural requirements for the biological activity of endothelin peptides, the solution structure of an ET_B selective agonist, ET-1[Cys-(Acm)^{1,15}, Ala^3,Leu^7,Aib^{11}], was investigated by ^1H NMR spectroscopy and molecular modelling. The structure is characterised by an α-helical conformation between residues Ser^5-His^{16} but is undefined at both the N and C termini. To date, neither the solution structures of linear modified peptides nor the effects of a methanol/water solvent system have been examined for endothelin or endothelin-like peptides. This structure plays an important role towards the design of endothelin receptor selective agonists and antagonists.

Key words: Endothelin; Molecular modeling; Nuclear magnetic resonance; Peptide solution structure

1. Introduction

The endothelins are a family of bicyclic 21-amino acid peptides. Endothelin-1 (ET-1) was first reported by Yanagisawa et al. [1], and was shown to be the most potent known vasoconstrictor. Subsequent studies have revealed more related mammalian subtypes, namely ET-2, ET-3 and (VIC) ET-β [2,3] as well as the reptilian sarafotoxins [4] isolated from the venom of burrowing asps. ET-1, ET-2 and ET-3 all appear to be distinct gene products, and ET-β appears to be the rat form of ET-2. Two major endothelin receptor subtypes, ET_A and ET_B, which are categorised according to their relative affinities, have been identified from bovine and rat lung respectively [5,6]. Human ET_A and ET_B receptors have also been cloned [7,8] and a third receptor subtype, ET_C, has been described [9]. The ET_A receptor has a higher specificity for ET-1 and ET-2 than for ET-3, and the ET_B receptor has approximately equal specificity for all the endothelins. These peptide families produce numerous biological responses and are implicated in a number of disease states on renal, cardiovascular, haemodynamics and endocrine function [10]. There have been many reports of structure-activity relationship studies and pharmacological evaluations of endothelin analogues and fragments [11–13]. The development of selective receptor agonists and antagonists plays an important role in providing therapeutic agents for the treatment of human diseases. To determine the important structural features, many research groups have studied solution conformations of endothelin peptides which show potential activity. In this paper, we present the solution structure of an endothelin B receptor selective agonist, ET-1[Cys(Acm)^{1,15},Ala^3,Leu^7,Aib^{11}] (Fig. 1) determined by molecular modelling based on ^1H nuclear magnetic resonance data.

*Corresponding author. Fax: (44) (131) 650 4743.
E-mail: i.h.sadler@ed.ac.uk

Abbreviations: DIANA, distance geometry algorithm for NMR applications; DQFCOSY, double quantum filtered correlation spectroscopy; DSA, dynamical simulated annealing; ET-1, endothelin-1; MD, molecular dynamics; NMR, nuclear magnetic resonance; NOESY, nuclear Overhauser effect correlation spectroscopy; RMSD, root mean square deviation; TOCSY, total correlation spectroscopy

2. Materials and methods

2.1. Peptide synthesis [14]

Peptide **LJP2** was synthesised by solid phase Fmoc chemistry (0.25 mmol scale) on an adapted ABI 430A Peptide Synthesiser using Wang resin as the solid supporter. All residues were incorporated by double-coupling protocols using HOCt active esters. The only exception was histidine which was coupled through its HOBt ester, due to increased racemisation with its HOCt ester. In each cycle, one cartridge containing 1.0 mmol Fmoc amino acid was used and the active ester was formed via the addition of 0.5 mmol DIC. The amino acid sidechain protections were: OtBu (Asp, Glu), tBu (Ser, Tyr), Boc (Lys), Trt (His), Acm (Cys). The Fmoc group was deprotected with 20% piperidine in DMF. The deprotection was monitored by an on-line UV system. Acetylation was carried out in a solution of 0.5 M acetic anhydride, 0.125 M DIEA and 0.2% HOBt in DMF. On completion of synthesis, the peptide was cleaved from the resin by treatment with a mixture of TFA:EDT:thioanisole:TIS:H_2O: (10:1:0.5:0.2:0.5). The crude peptide was precipitated from ether after removing the TFA in vacuo. The crude, fully reduced peptide was purified by a C_{18} semi-preparative column eluted with a linear gradient of 0.1% TFA/H_2O and an increasing concentration of 0.1% TFA/CH_3CN at 5 ml/min. The purified peptide, $C_{117}H_{178}N_{27}O_{34}S_2$, was characterised by electrospray MS ($[MH]^+$ found = 2568.6; calc. = 2569.2) and by different analytical HPLC conditions (RP C_{18}, Vydac C_{18} and Hichrom C_{18} columns). Amino acid analysis, after acid hydrolysis, gave the correct molar ratios of the constituent amino acids.

2.2. NMR spectroscopy

All NMR experiments were performed using a 5 mm inverse probehead on a Varian VXR 600S NMR spectrometer operating at a ^1H resonance frequency of 599.945 MHz. The peptide sample (5 mg) was dissolved in a 1:1 mixture of CD_3OH and H_2O (700 μl) except for amide proton exchange studies when the peptide sample was dissolved in a 1:1 mixture of CD_3OD and D_2O. The NMR experiments were carried out at 298 K except for studies where the effects of temperature were being monitored.

One-dimensional (1D) single pulse proton NMR spectra and two-dimensional (2D) phase-sensitive DQFCOSY [15], TOCSY [16] and NOESY [17] data sets were acquired with a presaturation delay of 1.5 s. An MLEV-17 'clean-tocsy' spin-lock pulse sequence was applied for a mixing time of 80 ms surrounded by two trim pulses of 2 ms each. The NOESY data were acquired with a 150 ms mixing time. The experiments were acquired with 32, 16 and 32 transients for each of 2×256 t_1 increments (hypercomplex acquisition) [18] into 2048 complex data points for the DQFCOSY, TOCSY and NOESY data respectively. Other acquisition parameters for all three data sets were as

PII S0014-5793(98)00239-7

follows: acquisition time, 0.146 s; spectral width, 7 kHz. Fourier transformation in F_2 was carried out without zero filling whereas data were zero filled to 1024 data points in F_1 prior to transformation. All the data sets were apodised in both dimensions using a shifted squared sinebell window function. The real FT was carried out on 1024×2048 data points. All the 2D spectra were acquired on a non-spinning sample. Variable temperature studies of the peptide sample (1 mg) were carried out using a standard 1D ^{1}H NMR pulse sequence. All spectra were referenced internally to the residual ^{1}H signal of CD_2HOH resonating at 3.30 ppm. Data were acquired and processed using the Varian VNMR software (Version 4.1).

2.3. Molecular modelling

Structure calculations were carried out using the Tripos molecular modelling software SYBYL (Version 6.1) [19]. NMR data used for structure calculations were imported into the TRIAD module of SYBYL. The NOESY data acquired with a mixing time of 150 ms were used to derive interproton distances. NOEs were classified into three categories of upper distance bounds according to their volume integral values: 2.8 Å (strong); 3.6 Å (medium); 5.0 Å (weak). The lower distance bound was in all cases set to the van der Waals distance of 1.8 Å. The threshold values of upper distance bounds were established based on known sequential distances of d_{NN} and $d_{\alpha N}$ [20]. Pseudo-atoms were introduced for protons which could not be stereospecifically assigned [21]. Amide protons which showed slow exchange rates from exchange studies were generally in the helical region of the peptide backbone. These were used as constraints with the relevant backbone carbonyl interatomic distances by introducing hydrogen bonds in the range 1.8–2.0 Å (H-O) and 2.7–3.0 Å (N-O) [22]. Torsional angle constraints, which were generated from the $^3J_{HN\alpha}$ coupling constants (<5.5 Hz), were applied in the $-90°$ to $-40°$ range.

Starting structures were built using SYBYL. The distance geometry program DIANA [23] was used to generate random starting structures. The 208 distance constraints obtained from the NOESY cross-peak volumes were used as input to DIANA. Eight constraints for hydrogen bonds and nine torsional angle constraints were also incorporated. During the DIANA calculation, atomic distances were constrained using the force constant $k_{NOE}=1$ kcal mol^{-1} Å^{-2} and torsions were constrained using $k_{Dihed.}=0.01$ kcal mol^{-1} deg^{-2}. DIANA was used to calculate 300 structures and the calculation produced 37 best structures along with 131 structurally important modified bounds. Output structures from the DIANA calculation were then constrained by these modified distance bounds. In these structures, interatomic distances were constrained using a higher force constant of $k_{NOE}=10$ kcal mol^{-1} Å^{-2}. Torsions were constrained using the same force constant. Structures were then subjected to 200 steps of conjugate-gradient energy minimisation.

Energy minimised structures were refined using a dynamical simulated annealing (DSA) protocol. DSA cycles proceeded with an annealing step at a temperature of 1000 K for a period of 5400 fs followed by an annealing period of 900 fs to a temperature of 100 K in a stepwise fashion. The Boltzmann scaling of atomic velocities was chosen from a random number seed. Ten cycles of heating and cooling were applied to each starting structure. The conformations obtained by DSA were further minimised with 200 steps of conjugate-gradient energy minimisation. The energy minimised conformations were subjected to a final molecular dynamics (MD) quenching calculation performed in the gas phase. The initial atomic velocities were chosen from a random distribution at 1000 K and the dynamic trajectory (100 fs) was followed for 20 ps in 1 fs steps. These calculations were carried out under NTV ensemble conditions with a 10 fs temperature coupling factor. The molecular dynamics calculations were repeated three times for each conformation using different random number seed values. Each set of conformers was averaged to obtain averaged conformations which were finally subjected to 500 steps of conjugate-gradient energy minimisation after the removal of all experimental energy barriers.

3. Results and discussion

Peptide **LJP2** was synthesised in our laboratory using a *newly developed* coupling reagent (HOCt) [14]. The coupling percentage of Peptide **LJP2** was greatly improved with this new coupling reagent and the crude peptide was afforded in very good purity according to HPLC analysis. Most of the pharmacological evaluations in the field of endothelin research have concentrated on endothelin and endothelin-like

Table 1
^{1}H chemical shifts[a] obtained for Peptide **LJP2** obtained in 1:1 aqueous methanol

	NH	αH αCH$_3$	βH βCH$_3$	γH γCH$_3$	δCH$_2$ δCH$_3$	εCH$_2$ εCH$_3$	Aromatics Others
1 C		4.30	3.16, 3.00				
2 S	8.75	4.54	3.90, 3.98				
3 A	8.66	4.28	1.43				
4 S	8.24	4.30	3.85, 3.90				
5 S	8.17	4.33	3.92, 4.00				
6 L	8.01	4.16	1.66, 1.66	1.66	0.88, 0.93		
7 L	7.93	4.16	1.60, 1.70	1.66	0.91, 0.87		
8 D	8.06	4.47	2.96, 2.86				
9 K	7.92	4.06	1.92, 1.60	1.43	1.65	2.93	+NH$_3$: 6.67, 6.70
10 E	8.11	4.06	2.17, 2.19	2.38, 2.59			
11 X[b]	8.14	1.54, 1.54					
12 V	7.55	3.72	2.06	0.97, 0.82			
13 Y	7.85	4.22	2.90, 2.90				2/6: 6.74, 3/5: 6.61
14 F	8.21	4.39	3.00, 3.25				2/6: 7.27, 3/5: 7.32 4H: 7.31
15 C	8.11	4.48	3.04, 3.04				
16 H	8.12	4.57	3.32, 3.25				2H: 8.58, 4H: 7.27
17 L	7.86	4.26	1.60, 1.60	1.53	0.79, 0.79		
18 D	8.30	4.62	2.75, 2.92				
19 I	7.69	4.09	1.71	0.74 1.01, 1.36	0.61		
20 I	7.86	4.15	1.76	0.80 1.08, 1.40	0.79		
21 W	8.03	4.65	3.17, 3.28				2H: 7.15, 4H: 7.54 5H: 7.03, 6H: 7.10 7H: 7.35, NH: 10.08

[a]Chemical shifts are referenced to the residual CD_2HOH signal at 3.3 ppm.
[b]X, α-aminoisobutyric acid.

	1	5	10	15	20
ET-1	C S C S S L M D K E C V Y F C H L D I I W				
Peptide **LJP2**	C S A S S L L D K E X V Y F C H L D I I W				

Fig. 1. Amino acid sequences of ET-1 and Peptide **LJP2**. The disulphide bridges of ET-1 are between C^1-C^{15} and C^3-C^{11}. Underlined residues are sites of differences from ET-1. The cysteine sidechains of Peptide **LJP2** were protected by the -CH_2-NH-CO-CH_3 (Acm) group. X denotes α-aminoisobutyric acid.

compounds and their truncated analogues. In this study we have concentrated on examining *linear* endothelin analogues of ET-1 by modifying crucial cysteine residues. These were replaced by either Ala or Aib (α-aminoisobutyric acid) residues. According to general peptide chemistry, Aib improves the stability and solubility of the peptide chain. In this case we made alterations to the inner disulphide bridge, replacing cysteine at position 3 by Ala and the other end of the disulphide bridge at position 11 by Aib. The sidechains of the outer disulphide bridge, Cys^1 and Cys^{15}, were protected by -CH_2-NH-CO-CH_3 (Acm) groups. The methionine at position 7, which is liable to oxidation, was replaced by leucine.

Peptide **LJP2** displayed well resolved, sharp NMR signals in the mixed solvent of aqueous methanol. The proton 1D and DQFCOSY, TOCSY and NOESY 2D spectra were acquired as described. Table 1 details the resonance assignments deduced for Peptide **LJP2** from these data. Almost all of the amino acid spin systems could be distinguished from one another in the TOCSY spectrum. Despite the low molecular mass of this peptide, a large number of negative nOes were observed in the 2D NOESY spectrum, which is a characteristic normally associated with folded proteins. The AMX spin systems, aromatics and multiple copies of the same amino acids were carefully delineated using the NOESY spectrum. The four aromatic residue spin systems were identified using the NOESY connectivities between β-protons and their aromatic ring proton resonances. The individual identification of aromatic resonance spin patterns were determined by direct comparison of the TOCSY and NOESY spectra. Sequence-specific resonance assignments were completed with complete identification of all the individual spin systems being simultaneously confirmed. Fig. 2 shows the sequential connectivity delineation along the backbone. Fig. 3 illustrates the nOe connectivities of Peptide **LJP2**. All the sidechain spin connectivities through αH signals were clearly observed in the TOCSY spectrum for all amino acid residues. Although weak cross-peaks were observed for methyl resonances of the α-aminoisobutyric acid, Aib^{11}, in the TOCSY spectrum, strong methyl resonances were observed in the NOESY spectrum. The $d_{\beta N}(i,i+1)$ and $d_{NN}(i,i+1)$ connectivities of neighbouring amino acid residues supported the reliability of the resonance assignments.

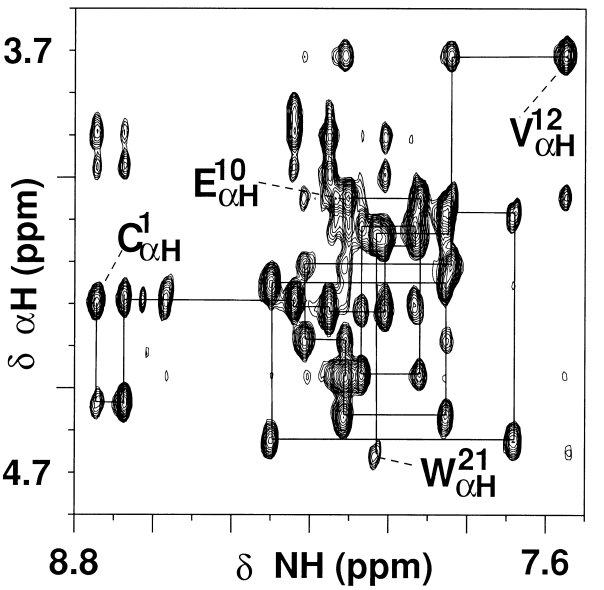

Fig. 2. Fingerprint (HN-H_α) region of the ^{1}H 2D NOESY NMR spectrum of Peptide **LJP2** at a mixing time of 150 ms. The backbone 'walk' is indicated together with selected residue assignments.

Evidence of secondary structure was obtained from long-

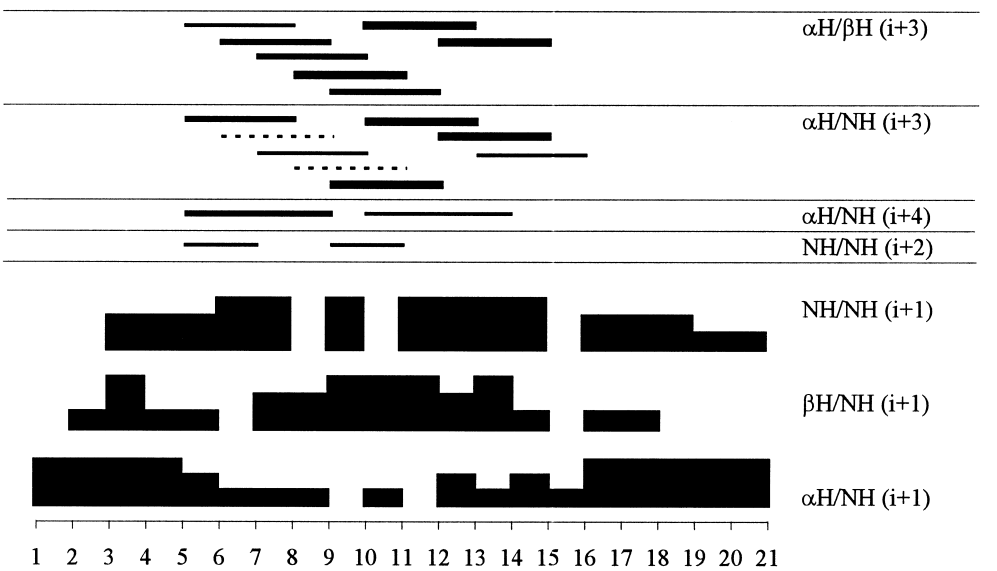

Fig. 3. Summary of interresidue nOe connectivities observed for Peptide **LJP2**. The thickness of the columns and bars is proportional to the nOe intensity. Broken bars represent overlapped nOe cross-peaks.

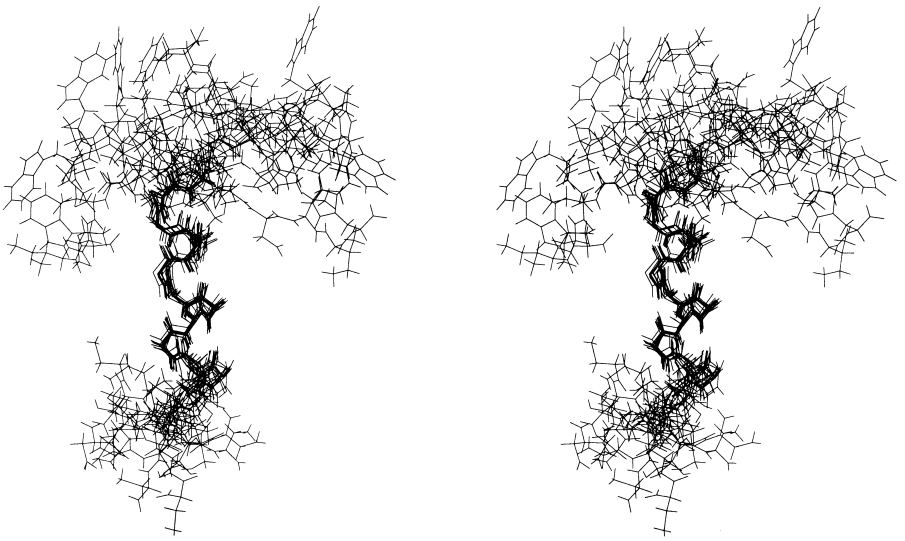

Fig. 4. Stereoview of 10 superimposed solution structures of Peptide **LJP2** based on the nOe data. The superimposition is shown as a best fit of the backbone for residues 5–16.

range connectivities observed in the NOESY spectrum. The fingerprint region of the NOESY spectrum showed clear $d_{\alpha N}(i,i+3)$ connectivities for S^5/D^8, K^9/V^{12}, V^{12}/C^{15}, F^{14}/L^{17}, some overlapping cross-peaks for L^6/K^9, D^8/X^{11} and weak connectivities of E^{10}/F^{14} and Y^{13}/H^{16}. The methyl resonance of Aib^{11} also showed strong long-range connectivity to $F^{14}NH$. The aliphatic region of the NOESY spectrum showed $d_{\alpha\beta}(i,i+3)$ cross-peaks, S^5/D^8, L^6/K^9, L^7/E^{10}, D^8/X^{11}, K^9/V^{12}, E^{10}/Y^{13} and V^{12}/C^{15}, supporting evidence for an α-helical segment between S^5-H^{16}. The prominent connectivity patterns of $d_{\alpha N}(i,i+n)$, $d_{NN}(i,i+1)$ and $d_{\alpha\beta}(i,i+3)$ confirmed the α-helical character of Peptide **LJP2**. Small $^3J_{NH\alpha}$ coupling constants (∼4 Hz) measured from the 1D ^1H NMR spectrum were also consistent with an α-helical character.

The temperature dependence of backbone amide proton chemical shifts was measured over the temperature range 290–313 K. A structured state was apparent from the very small temperature gradient of D^8 $\Delta\delta/\Delta T = -0.7$ ppb/C. Small temperature coefficients of −1.8 ppb/C for Y^{13} and −3.4 ppb/C for K^9 and H^{16} indicated shielding from solvent exchange of the amide protons of residues between 9 and 16. This suggested that amide protons in the helical region were involved in hydrogen bonding. The remaining parts of Peptide **LJP2**, especially the C-terminal region beyond H^{16}, showed a series of strong $d_{\alpha N}(i,i+1)$ NOEs and larger $^3J_{NH\alpha}$ coupling constants for I^{19}, I^{20} and W^{21} (∼7 Hz).

These qualitative observations were combined with the results from the quantitative structure calculations describe earlier. These structures clearly revealed the α-helical character between residues 5 and 16. Fig. 4 shows a representative family of 10 structures resulting from a combination of DIANA, DSA and energy minimisation calculations. The final atomic RMSD for all atoms in the helical region (residues 6–15) was found to be 1.95 ± 0.32 Å, compared to backbone only atoms for which the final RMSD was found to be 0.63 ± 0.22 Å. The ordered sidechain groups adopted a stable conformation as evidenced by numerous interresidue nOe constraints observed for this region. It was possible to observe the extension of the helix form one residue either side for some of the modelled structures. This was clearly confirmed by weak long-range cross-peaks observed in the NOESY spectrum.

NMR structures of ET-1 in *aqueous* media define the helical structural region from Lys^9 to Cys^{15} and in some cases this has been shown to extend to Leu^{17} [24,25]. Peptides are naturally formed in aqueous environments and water could therefore have been used as the NMR solvent in the present study. By way of contrast, less polar solvents, such as methanol or TFE, tend to induce more structure in peptides because of the weaker capacity of the solvent to engage in hydrogen bonding with the peptide. In our studies, water alone was found to precipitate peptides of a similar sequence to that under investigation in the current study. A more suitable NMR solvent was found to be a 1:1 mixture of CD_3OH:H_2O. This mixed solvent system is frequently used in our laboratory for analysis by HPLC. Our studies of the solution structure of synthetic ET-1 (synthesised in this laboratory) in the same mixed solvent system showed the α-helix to lie between residues Lys^9 and His^{16} [26]. Removal of the disulphide constraints and introduction of the amino acid residues Ala and Aib lengthens the α-helix by one turn compared to the α-helix of ET-1. Contradictory reports exist of the conformation of the biologically important C-terminal region of endothelin and endothelin-related peptides, but most studies have been unable to describe in detail the tail region. Our studies failed to reveal any defined structural features at either the N or C terminus. This is reflected in both the total atom RMSD for residues 1–21 of 5.68 ± 1.20 Å and the backbone atom RMSD for the same residues of 4.04 ± 0.91 Å. These figures are consistent with disordered N and C termini. The $^3J_{NH\alpha}$ couplings measured for these regions of Peptide **LJP2** were consistent with conformational averaging. The H-D exchange studies of similar peptides of the same length and with identical C-terminal residues showed somewhat slower amide protons exchange rates for the last three residues, I^{19}, I^{20} and W^{21}. This indicates poor solvent accessibility to the amide protons in the tail region. The calculated structures obtained for Peptide **LJP2** remain within one family of conformations and the level of agreement obtained between structures, especially in the heli-

cal region, demonstrated the ordered conformation in which a helical region, extending from Ser^{5} to His^{16}, exists.

Numerous studies have been carried out using synthetic analogues and fragments of endothelin with each portion of the peptide being examined for its relative importance in receptor binding and functional activities. In general, full length bicyclic analogues appear to be required for ET_A binding whilst linear and truncated analogues have proved to be ET_B receptor selective. The linear endothelin analogue ET-1[1,3,11,15-Ala], in which all cysteines are replaced by alanines, did not require the presence of the disulphide bridges for binding to the rat cerebellum (ET_B receptor) [27,28] but it was functionally inactive in the rat aorta and mesenteric bed (ET_A receptor) [29].

In this study, Peptide **LJP2**, in which the inner disulphide bridge positions 3 and 11 were replaced with Ala and Aib respectively, shows potent agonist activity in the rat cerebellum (ET_B). The results observed for similar *linear* ET-1 analogues suggest that the two disulphide bridges are critical for ET_A receptor binding but not for ET_B receptor binding [30–32]. Nakajima et al. [33] reported that the replacement in ET-1 of Met^{7} by Leu^{7} caused no loss in agonist activity in rat pulmonary artery (ET_B). In our studies, the linear ET-1 analogues, synthesised by replacing the methionine at position 7 with norleucine or leucine, showed similar results for receptor binding and functional activity [34]. However, with leucine at position 7, the functional activity at the ET_B receptor site was slightly reduced for some analogues [34].

In conclusion we have shown, by NMR and molecular modelling, that a synthetic linear modified derivative of the ET_B receptor binding peptide ET-1, namely Peptide **LJP2** (ET-1[$Cys(Acm)^{1,15}$,Ala^{3},Leu^{7},Aib^{11}]), folds into an α-helix in a 1:1 water/methanol mixed solvent solution. Our studies also demonstrate that the disulphide bridges present in ET-1 are crucial neither for maintaining secondary structural features nor for affecting ET_B receptor binding activity.

Acknowledgements: We are grateful to the University of Ruhuna, the Commonwealth Association and the British Council for the Research Assistantship to C.M.H., the EPSRC for access to 600 MHz NMR facilities in Edinburgh and to the Wellcome Trust for Molecular Modelling facilities. We also thank Parke Davis Pharmaceuticals for financial support and bioassays and Brian Wigham and Kevin Shaw for technical assistance with the synthesis.

References

[1] Yanagisawa, M., Kurihara, H., Kimura, S., Tomobe, Y., Kobayashi, M., Mitsui, Y., Yazaki, Y., Goto, K. and Masaki, T. (1988) Nature 332, 411–415.
[2] Itoh, Y., Yanagisawa, M., Ohkubo, S., Kimura, C., Kosaka, T., Inoue, A., Ishida, N., Mitsui, Y., Onda, H. and Fujino, M. (1988) FEBS Lett. 231, 440–444.
[3] Saida, K., Mitsui, Y. and Ishida, N. (1989) J. Biol. Chem. 264, 14613–14616.
[4] Bdolah, A., Wollberg, Z., Fleminger, G. and Kochva, E. (1989) FEBS Lett. 256, 1–3.
[5] Arai, H., Hori, S., Aramori, I., Ohkubo, H. and Nakanishi, S. (1990) Nature 348, 730–732.
[6] Sakurai, T., Yanagisawa, M., Takuwa, Y., Miyazaki, H., Kimura, S., Goto, K. and Masaki, T. (1990) Nature 348, 732–735.
[7] Kimura, S., Kasuya, Y., Sawamura, T., Shinimi, O., Sugita, Y., Yanagisawa, M., Goto, K. and Masaki, T. (1989) J. Cardiovasc. Pharmacol. 13, S5–S7.
[8] Kitamura, K., Yukawa, T., Morita, S., Ichiki, Y., Eto, T. and Tanaka, K. (1990) Biochem. Biophys. Res. Commun. 170, 497–503.
[9] Karne, S., Jayawickreme, C.R. and Lerner, M.R. (1993) J. Biol. Chem. 268, 19126–19133.
[10] Doherty, A.M. (1992) J. Med. Chem. 35, 1493–1508.
[11] Kimura, S., Kasuya, Y., Sawamura, T., Shinmi, O., Sugita, Y., Yanagisawa, M., Goto, K. and Masaki, T. (1988) Biochem. Biophys. Res. Commun. 156, 1182–1186.
[12] Huggins, J.P., Pelton, J.T. and Miller, R.C. (1993) Pharmacol. Ther. 59, 55–123.
[13] Cody, W.L. and Doherty, A.M. (1995) Biopolymers 37, 89–104.
[14] Ramage, R., Biggin, G.W., Brown, A.R., Comer, A., Davidson, A., Draffan, L., Jiang, L., Morton, G., Robertson, N., Shaw, K.T., Tennant, G., Urquhart, K. and Wilkin, J. (1996) in: Proceedings of the Fourth International Symposium: Innovation and Perspectives in Solid Phase Synthesis and Combinatorial Chemical Libraries, September 1996, Edinburgh (Epton, R., Ed.), pp. 1–10, Mayflower Scientific, Birmingham.
[15] Shaka, A.J. and Freeman, R. (1983) J. Magn. Reson. 51, 169–173.
[16] Bax, A. and Davis, D.G. (1985) J. Magn. Reson. 65, 355–360.
[17] Kumar, A., Ernst, R.R. and Wüthrich, K. (1980) Biochem. Biophys. Res. Commun. 95, 1–6.
[18] States, D.J., Haberkorn, R.A. and Ruben, D.J. (1982) J. Magn. Reson. 48, 286–292.
[19] Tripos Molecular Modelling Software, SYBYL version 6.1, Tripos Associates, St. Louis, MO.
[20] Billeter, M., Braun, W. and Wüthrich, K. (1982) J. Mol. Biol. 155, 321–346.
[21] Wüthrich, K., Billeter, M. and Braun, W. (1983) J. Mol. Biol. 169, 949–961.
[22] Williamson, M.P., Havel, T.F. and Wüthrich, K. (1985) J. Mol. Biol. 182, 295–315.
[23] Güntert, P., Braun, W. and Wüthrich, K. (1991) J. Mol. Biol. 217, 517–530.
[24] Ragg, E., Mondelli, R., Penco, S., Bolis, G., Baumer, L. and Guaragna, A. (1994) J. Chem. Soc. Perkin Trans. 2, 1317–1326.
[25] Krystek, S.R., Bassolino, D.A., Novotny, J., Chen, C., Marschner, T.M. and Andersen, N.H. (1991) FEBS Lett. 281, 212–218.
[26] Hewage, C.M., Jiang, L., Parkinson, J.A., Ramage, R. and Sadler, I.H. (1997) J. Peptide Sci. 3, 415–428.
[27] Kitazumi, K., Shiba, T., Nishiki, K., Furukawa, Y., Takasaki, C. and Tasaka, K. (1990) FEBS Lett. 260, 269–272.
[28] Randall, M.D., Douglas, S.A. and Hiley, C.R. (1989) Br. J. Pharmacol. 98, 685–699.
[29] Hiley, C.R., Jones, C.R., Pelton, J.T. and Miller, R.C. (1990) Br. J. Pharmacol. 101, 319–324.
[30] Ihara, M., Saeki, T., Fukuroda, T., Kimura, S., Ozaki, S., Patel, A.C. and Yano, M. (1992) Life Sci. 51, 47–52.
[31] James, A.F., Urade, Y., Webb, R.L., Karaki, H., Umemura, I., Fugitani, Y., Oda, K., Okada, T., Lappe, R.W. and Takai, M. (1993) Cardiovasc. Drug Rev. 11, 253–270.
[32] Saeki, T., Ihara, M., Fukuroda, T. and Yano, M. (1992) Biochem. Int. 28, 305–312.
[33] Nakajima, K., Kubo, S., Kumagaye, S., Nishio, H., Tsunemi, M., Inui, T., Kuroda, H., Chino, N., Watanabe, T.X., Kimura, T. and Sakakibara, S. (1989) Biochem. Biophys. Res. Commun. 163, 424–429.
[34] Jiang, L. (1996) PhD Thesis, University of Edinburgh.